Journal of Ceramic Processing Research. Vol. 19, No. 1, pp. 54~64 (2018)

J O U R N A L O F
Ceramic Processing Research

A study on the wear characteristics of ZrO_2 monoliths and ZrO_2/SiC composites

Kwang-Ho Lee[a] and Ki-Woo Nam[b,*]
[a]*Daewoo Shipbuilding & Marine Engineering Co., Ltd., Gyeongsangnam-do 53302, Korea*
[b]*Department of Materials Science and Engineering, Pukyong National University, Busan 48547, Korea*

We was evaluated the wear characterization of monolithic ZrO_2 ceramics and ZrO_2/SiC composite ceramics. The test specimen was prepared by hot-press sintering at 35 MPa and 1723 K in a vacuum condition for 1 h. We were carried out bending test, the Vickers hardness and the abrasion test. The bending strength of as-received Z specimen was about twice higher than that of as-received ZS specimen. Average hardness of heat treated Z specimen is about 2-16% higher than that of as-received specimen. However, average hardness of as-received ZS specimen was similar to that of as-received Z specimen, average hardness of heat treated ZS specimen is 11-40% smaller than that of as-received ZS specimen. The friction coefficient of as-received Z specimen and heat treated Z specimen were similar as a whole. Friction coefficient of ZS specimen was inversely proportional to the Vickers hardness. Wear loss of Z and ZS specimens were increased according to the Vickers hardness decreases.

Key words: ZrO_2, Heat treatment, Bending strength, Vickers hardness, Wear, Friction coefficient, Wear loss.

Introduction

Ceramic has been actively studied as a high-temperature structural material, because it has excellent heat, corrosion and abrasion resistance, and has excellent properties that metallic materials lack. Using these characteristics is expected to have a great effect on energy saving by application to the heat cycle engine, such as the gas turbine or automobile engine. However, ceramics generally have low fracture toughness, low reliability, and poor processability. In order to overcome these shortcomings, many researchers have made various proposals to improve the reliability of ceramics. Currently, many researchers are studying the strength improvement of ceramic with the ability of crack healing by the addition of silicon carbide (SiC) [1-9]. That is, silicon carbide was added to silicon nitride (Si_3N_4) and alumina (Al_2O_3), and then heat-treated. Researches on crack healing and strength increase by the formation of SiO_2, which is a crack healing material, have been actively carried out.

Researches on crack healing and strength increase by adding silicon carbide to zirconia (ZrO_2) have been conducted, and reliability evaluation has also been conducted [10-13]. Zirconia (ZrO_2, Zirconia) has ease of sintering, high heat resistance, and low thermal conductivity, compared to other ceramics. It is also resistant to rapid temperature change, and is highly resistant to acidic and alkaline solutions. In addition, due to its excellent material properties, such as high strength, high hardness, and abrasion resistance, it has good physical and mechanical properties, and has attracted attention as a heat resistant material. ZrO_2 adopts a monoclinic crystal structure at room temperature, and transitions to tetragonal and cubic structure at higher temperatures [11, 14]. This substance can be manufactured in high toughness and high-strength ceramic. Excessive transition has been reported to possibly lower the strength.

Identifying and evaluating the mechanical and wear properties of ceramics is very important as basic data for the design, manufacture, and development of materials [15-18]. There are many studies on the wear characteristics of zirconia-coated materials [19-22], and on evaluating the wear characteristics of composite ceramics with silicon carbide added to zirconia [23, 24].

In this study, yttria-stabilized ZrO_2 monoliths ceramic, which is widely used in ceramic balls, etc., and ZrO_2/SiC composite ceramic with 10 wt.% SiC, which has crack-healing ability, were sintered. These were made into specimens, and heat-treated for (1, 5, and 10) h at (1,073 and 1,173) K. These test specimens were evaluated for their mechanical properties and wear characteristics, and the results were reviewed.

Materials and Test Methods

The ZrO_2 powder used in this study was TZ-3Y-E including stabilizer Y_2O_3 3 mol.% (0.26 μm mean particle size, Tosho Co., Japan). The SiC powder was

*Corresponding author:
Tel : +82-51-629-6358
Fax: +82-51-629-6353
E-mail: namkw@pknu.ac.kr

Table 1. Batch composition and processing.

Specimen	Z	ZS
Batch composition (wt.%)	100 wt.% ZrO_2	90 wt.% ZrO_2, 10 wt.% SiC
Hot Pressing	30 MPa, 1723 K 1 hour in vaccum	30 MPa, 1723 K 1 hour in vaccum
Heat treatment	1073 K and 1173 K from 1 to 10 hours in air	1073 K and 1173 K from 1 to 10 hours in air
Relative Density (%)	100.17	100.90

ultrafine powder (0.27 μm mean particle size, Wako Pure Chemical Industries, Ltd., Japan). Ethanol was added to this mixture, and was completely blended for 24 h. The mixture was placed in desiccators to extract the solvent, and to make a dry powder mixture. Plates were sintered in vacuum for 1 h via a hot press under 30 MPa at 1,723 K. Hereafter, ZrO_2 specimen and ZrO_2/SiC composite specimen are called the Z specimen and ZS specimen, respectively. Table 1 shows the composition of the specimens. Specimens for wear test were heat-treated. The heat-treatment was carried out in air for (1, 5 and 10) h at (1,073 and 1,173) K. All fracture tests were performed on a three-point loading system with a span of 16 mm at room temperature. The cross-head speed in the monotonic test was 0.5 mm/min. Hardness was measured using a Vickers hardness tester (HV-114, Mitutoyo). The specimens were measured for 10 s with indentation loads of 9.8 N. The type of wear tester (BRW140, Neoplus) was a "block on ring". This equipment consists of a circular plate ring-shaped counterpart material that rotates during the test, and a rectangular-shaped specimen that is under constant load, in order to maintain contact with the counterpart material. The counterpart material was SKD 11 of 35 mm diameter and 7 mm thickness. The test conditions were as follows; (1) the rotation speed of the ring was 50 rpm; (2) the loads were (9.8 and 24.5) N; (3) the total wear distance was 500 m; and (4) the tests were performed at room temperature in a dried condition. To obtain high reliability, 55,000 data that were obtained at 10 data per second were used.

Results and Discussion

Fig. 1 shows the bending strengths for the as-received Z specimens, which are ZrO_2 monoliths ceramics, and as-received ZS specimens, which are ZrO_2/SiC composite ceramics. Table 2 shows the mean, standard deviation (Std), and coefficient of variation (COV) according to mathematical statistics. The bending strength of the as-received Z specimen is about twice as high as that of the as-received ZS specimen. It is evident that the variation coefficient of Z specimen is smaller than that of ZS specimen, and the variation of bending strength is smaller. However, in the previous study, ZS specimens exhibited crack healing properties that were not found in Z specimens, due to the addition of SiC.

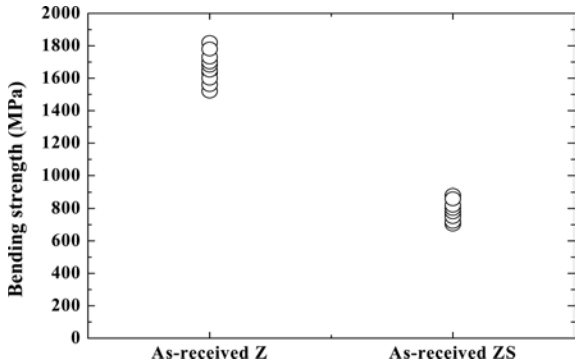

Fig. 1. Bending strength of as-received Z and ZS specimen.

Table 2. Mean, standard deviation (Std) and coefficient of variation (COV) by arithmetic statistics for bending strength of as-received specimen.

Specimen	Z specimen	ZS specimen
Mean	1668	779
Std	94.2	60.9
COV	0.056	0.078

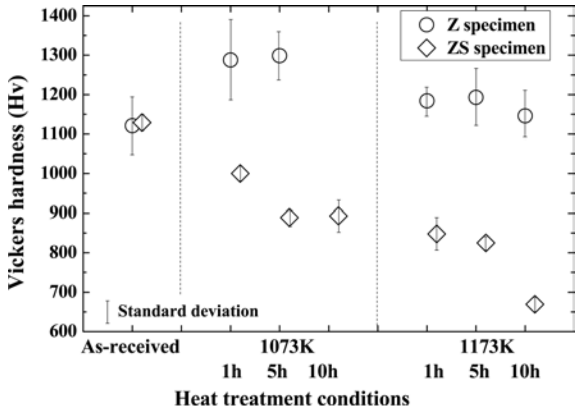

Fig. 2. Vickers hardness according to heat treatment conditions of Z and ZS specimen.

Fig. 2 shows the Vickers hardness of the as-received specimen and heat-treated Z and ZS specimens, respectively. The figure also shows the standard deviation. Tables 3 and 4 show the mean, standard deviation (Std), and coefficient of variation (COV) according to mathematical statistics on the Vickers hardness of Z and ZS specimens. The Vickers hardness of Z and ZS specimens all showed a variance, although there was a difference in degree. The mean hardness of the heat-treated Z specimen was (2-16) % higher than the as-received Z specimen. However, the mean hardness of the as-received ZS specimen was similar to that of the as-received Z specimen, but the mean hardness of the heat-treated ZS specimen was (11-40) % smaller than the as-received ZS specimen.

Table 3. Mean, standard deviation (Std) and coefficient of variation (COV) by arithmetic statistics for Vickers hardness of Z specimen.

Specimen	As-received	1073K-1h	1073K-5h	1173K-1h	1173K-5h	1173K-10h
Mean	1121	1288	1299	1184	1193	1146
Std	73.50	102.60	61.98	36.56	74.42	59.47
COV	0.066	0.080	0.048	0.031	0.062	0.052

Table 4. Mean, standard deviation (Std) and coefficient of variation (COV) by arithmetic statistics for Vickers hardness of ZS specimen.

Specimen	As-received	1073K-1h	1073K-5h	1073K-10h	1173K-1h	1173K-5h	1173K-10h
Mean	1129	1000	889	893	848	825	669
Std	22.92	21.50	21.02	39.33	42.48	16.13	18.32
COV	0.020	0.022	0.024	0.044	0.050	0.020	0.027

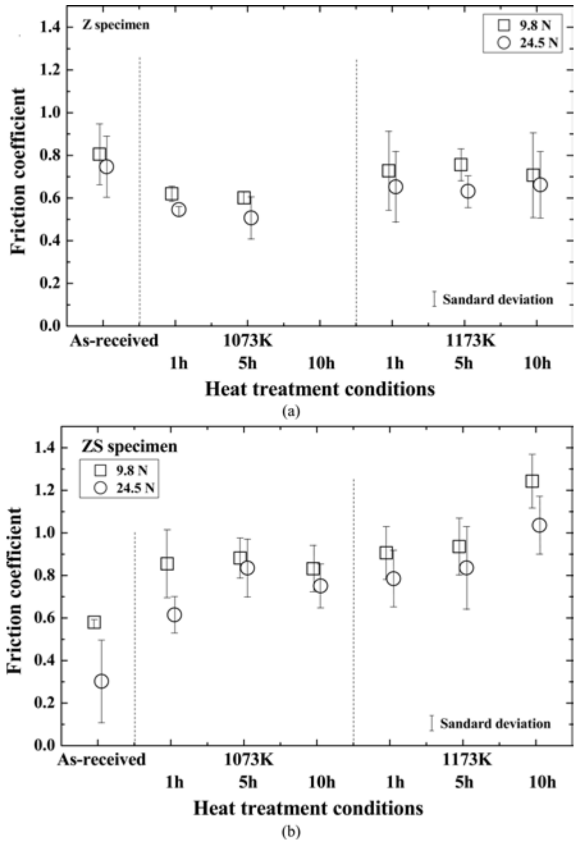

Fig. 3. Friction coefficient according to heat treatment conditions. (a) Z specimen, (b) ZS specimen.

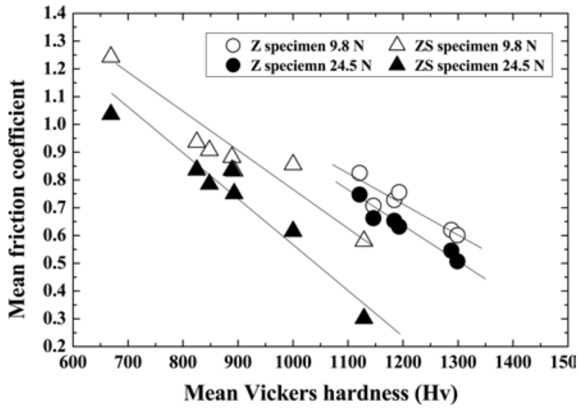

Fig. 4. Relationship of between friction coefficient and Vickers hardness.

This is the effect of glassy SiO_2 [5], which contributes to the crack healing created on the surface by heat-treatment.

Fig. 3(a) and (b) show the coefficient of friction of the Z and ZS specimens according to the heat-treatment conditions, respectively. Tables 3 and 4 show the mean and standard deviation of Z and ZS specimens, respectively.

In Fig. 3, the open square (□) and open circle (○) depict the results of the wear tests with loads of (9.8 and 24.5) N, respectively. The friction coefficient of the Z and ZS specimens was slightly higher for the 9.8 N. In Fig. 3(a), the as-received specimen was slightly larger than the friction coefficient of the heat-treated specimen. 1,173 K was higher than 1,073 K. Z specimens showed different friction coefficients, depending on the heat-treatment temperature. This is judged to be the effect of the oxide. In Fig. 3(b), the friction coefficient of the as-received specimen was the smallest, and the 1,173 K-10 h specimen was the largest. Except for the 1,073 K-1 h specimen by 24.5 N load and the 1,173 K-10 h specimen by (9.8 and 24.5) N load, the other coefficients of friction were similar.

The coefficient of friction of the ZS specimen was inversely proportional to the Vickers hardness. That is, as the Vickers hardness decreases, the coefficient of friction increases. This Z-specimen is monolithic, and does not produce glassy SiO_2 on the surface due to heat-treatment, but ZS specimen is made of glassy SiO_2, which is known as a crack-healing material by the addition of SiC.

Fig. 4 shows the relationship between the mean Vickers hardness and mean friction coefficient. The circle symbol represents the Z specimen, while the triangle symbol represents the ZS specimen. The white and black symbols indicate wear loads of (9.8 and 24.5) N, respectively. The friction coefficients of Z and ZS specimens were inversely related to the Vickers hardness. This is similar to that obtained with Si_3N_4/SiC [25]. The friction coefficient of the small load 9.8

Table 5. Friction coefficient of Z specimen.

Z Specimen	9.8 N	24.5 N
As-received	0.805 ± 0.143	0.747 ± 0.143
1073K-1h	0.620 ± 0.036	0.546 ± 0.014
1073K-5h	0.601 ± 0.027	0.507 ± 0.099
1173K-1h	0.728 ± 0.185	0.653 ± 0.165
1173K-5h	0.756 ± 0.075	0.632 ± 0.077
1173K-10h	0.707 ± 0.199	0.662 ± 0.156

Table 6. Friction coefficient of ZS specimen.

ZS Specimen	9.8 N	24.5 N
As-received	0.580 ± 0.013	0.302 ± 0.194
1073K-1h	0.855 ± 0.160	0.615 ± 0.086
1073K-5h	0.882 ± 0.094	0.835 ± 0.136
1073K-10h	0.832 ± 0.109	0.751 ± 0.103
1173K-1h	0.906 ± 0.124	0.785 ± 0.133
1173K-5h	0.936 ± 0.134	0.836 ± 0.194
1173K-10h	1.243 ± 0.126	1.036 ± 0.136

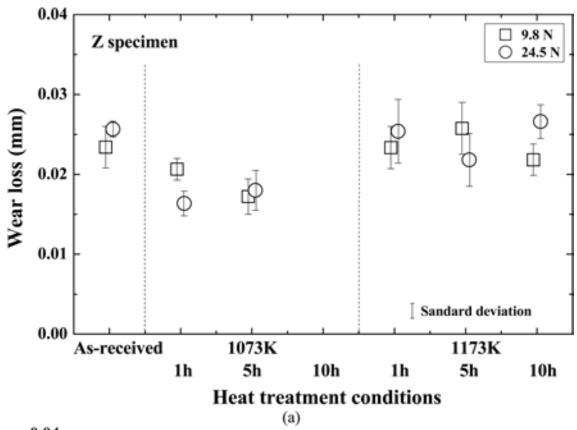

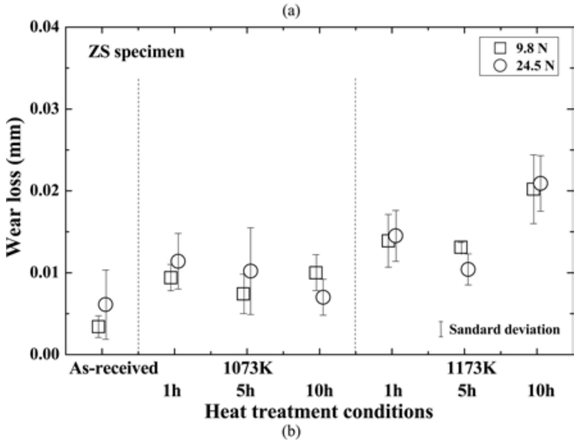

Fig. 5. Wear loss according to heat treatment conditions. (a) Z specimen, (b) ZS specimen.

Table 7. Wear loss of Z specimen.

Z Specimen	9.8 N	24.5 N
As-received	0.02340 ± 0.00260	0.02566 ± 0.00100
1073K-1h	0.02064 ± 0.00136	0.01635 ± 0.00155
1073K-5h	0.01721 ± 0.00221	0.01800 ± 0.00250
1173K-1h	0.02334 ± 0.00266	0.02539 ± 0.00399
1173K-5h	0.02575 ±0.00325	0.02180 ± 0.00330
1173K-10h	0.0218 ± 0.00200	0.02660 ± 0.00210

Table 8. Wear loss of ZS specimen.

ZS Specimen	9.8 N	24.5 N
As-received	0.00340 ± 0.00132	0.0061 ± 0.00423
1073K-1h	0.00940 ± 0.00160	0.0114 ± 0.00340
1073K-5h	0.00741 ± 0.00240	0.0102 ± 0.00530
1073K-10h	0.01000 ± 0.00220	0.0070 ± 0.00473
1173K-1h	0.0139 ± 0.00929	0.0145 ± 0.00260
1173K-5h	0.01310 ± 0.00060	0.0104 ± 0.00190
1173K-10h	0.02020 ± 0.00420	0.0209 ± 0.00340

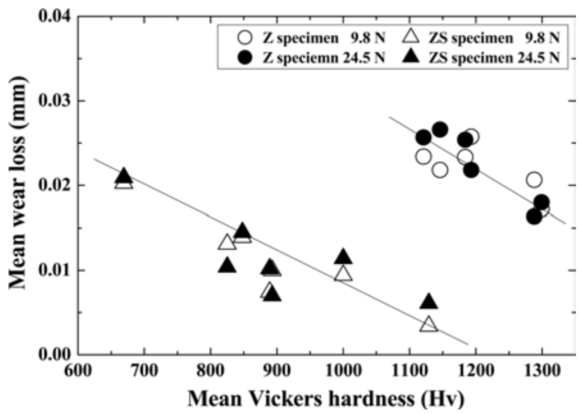

Fig. 6. Relationship of between wear loss and Vickers hardness.

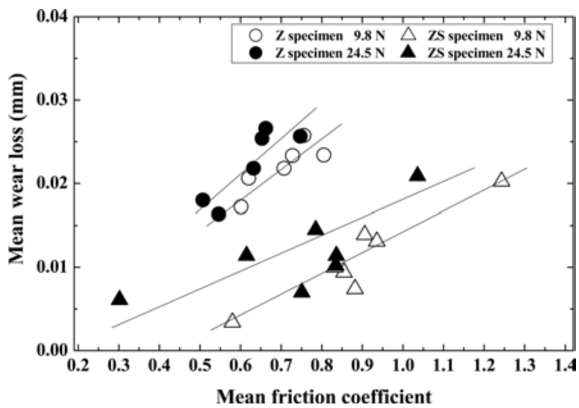

Fig. 7. Relationship of between friction coefficient and wear loss.

N was greater than that of the 24.5 N, despite the lubrication action of surface oxides. However, the friction coefficient of large load 24.5 N was reduced, because of removing the oxide on the surface, and abrasion of the surface of the hard ceramic. The ZS specimen, in which the glassy SiO_2 is forming, shows a larger difference in friction coefficient between the two loads. This is because the thickness of the oxide layer becomes thicker as the heat-treatment temperature becomes higher, or the heat-treatment time becomes longer [17].

Fig. 5 shows the wear loss of the Z and ZS specimens according to the heat-treatment conditions,

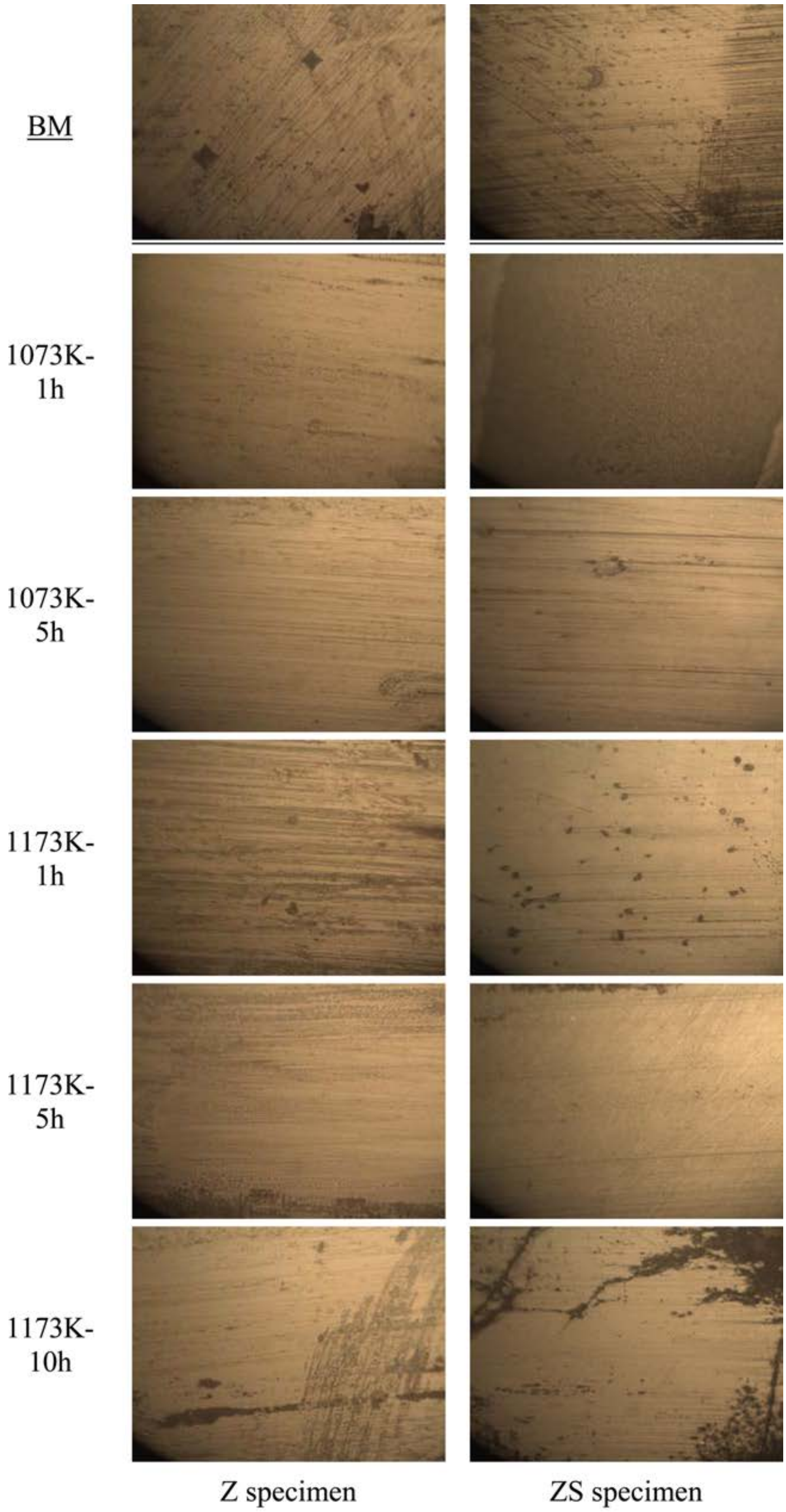
BM
1073K-1h
1073K-5h
1173K-1h
1173K-5h
1173K-10h
Z specimen
ZS specimen

(a)

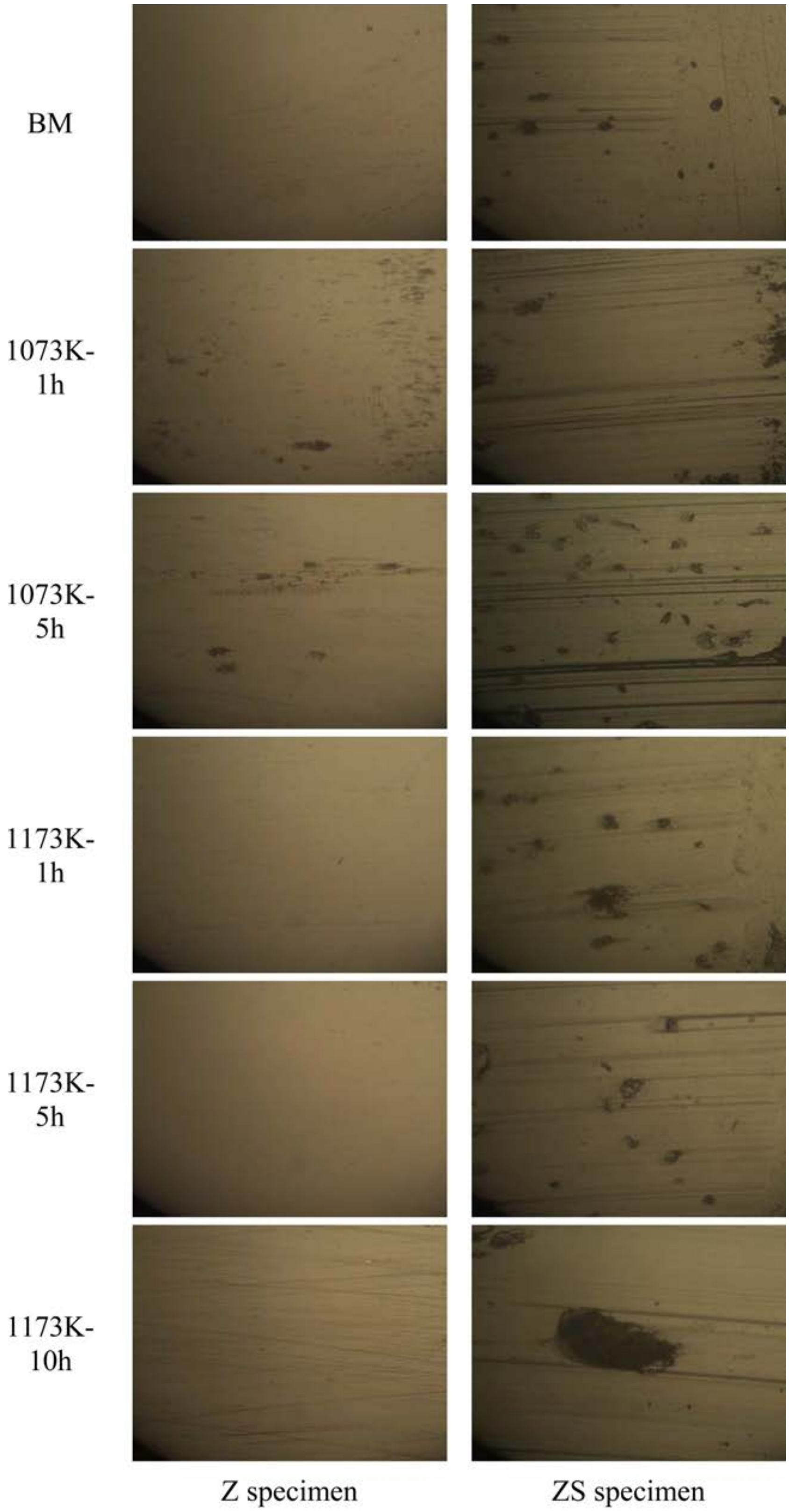

(b)

Fig. 8. Optical microscope image after wear test. (a) 9.8 N, (b) 24.5 N.

respectively. Tables 7 and 8 also show the mean and standard deviation. The open square (□) depicts the wear load of 9.8 N, while the open circle (○) depicts the wear load of 24.5 N. Fig. 5(a) and (b) show that the wear load does not significantly affect the wear loss of the ZS specimen. In detail, since the Z specimen (Fig. 5(a)) is formed with a small oxide, the difference due to the load is small. However, the ZS specimen (Fig. 5(b)) was slightly larger overall on the wear load of 24.5 N, because of SiO_2 formation. The wear loss tended to be similar to the friction coefficient.

Fig. 6 shows the relationship between the mean Vickers hardness and mean wear loss. The circle symbol represents the Z specimen, while the triangle symbol represents the ZS specimen. Meanwhile the white symbol indicates a wear load of 9.8 N, and the black symbol a wear load of 24.5 N. Wear loss of Z and ZS specimens was inversely related to Vickers

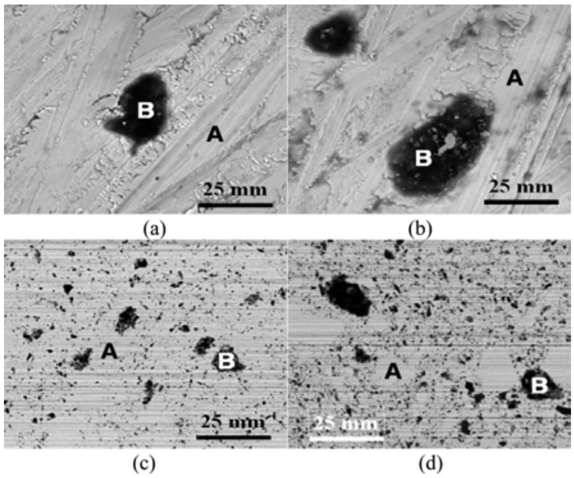

Fig. 9. SEM of wear scars. (a) As-received Z specimen, (b) 1073K-1h Z specimen, (c) As-received ZS specimen, (d) 1073K-1h ZS specimen.

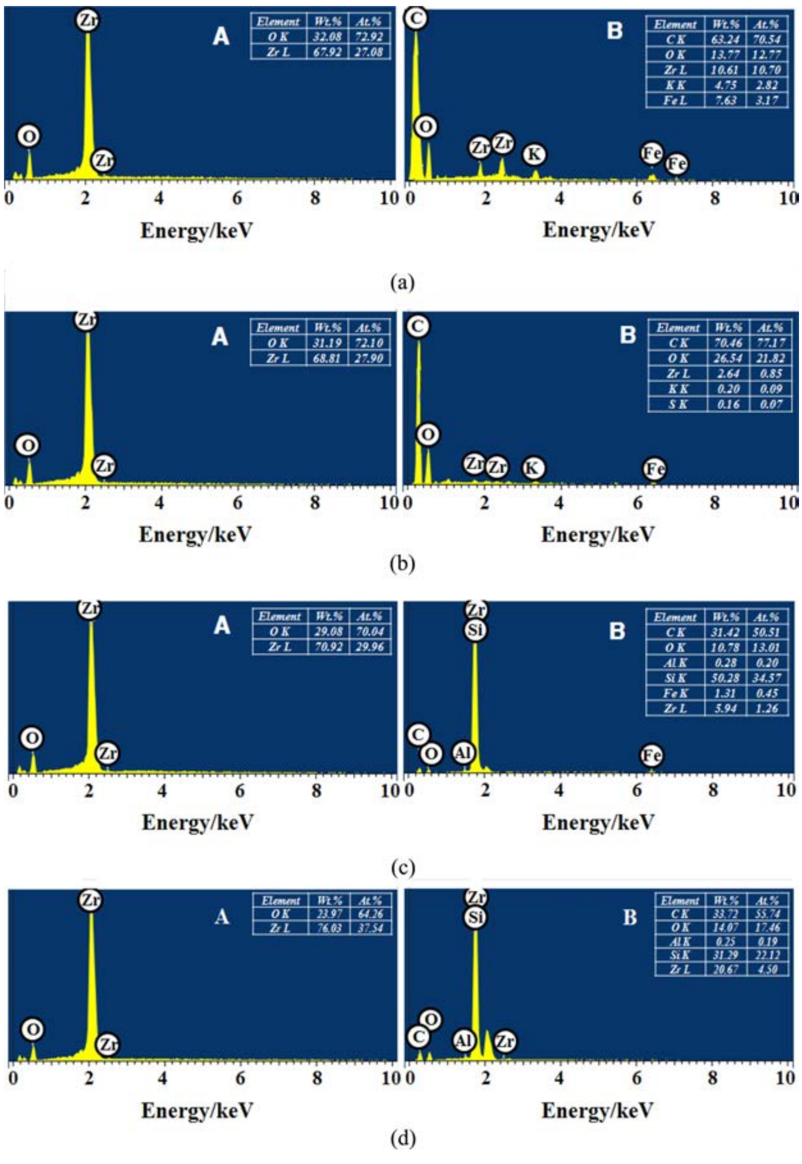

Fig. 10. EDX results of light regions (denoted as A) and dark regions (denoted as B). (a) As-received Z specimen, (b) 1073K-1h Z specimen, (c) As-received ZS specimen, (d) 1073K-1h ZS specimen.

hardness. However, unlike the coefficient of friction, there was no effect by wear load.

Fig. 7 shows the relationship between the mean Vickers hardness and mean wear loss. The circle symbol represents the Z specimen, while the triangle symbol represents the ZS specimen; meanwhile, the white and black symbols indicate wear loads of (9.8 and 24.5) N, respectively. The wear loss of the Z and ZS specimens was proportional to the friction coefficient. The wear loss of each specimen was increased by the load of 24.5 N. The ZS specimen was lubricated by SiO_2 formed on the surface, and the amount of wear was small, but the friction coefficient was large.

Fig. 8 shows the optical microscope images of the

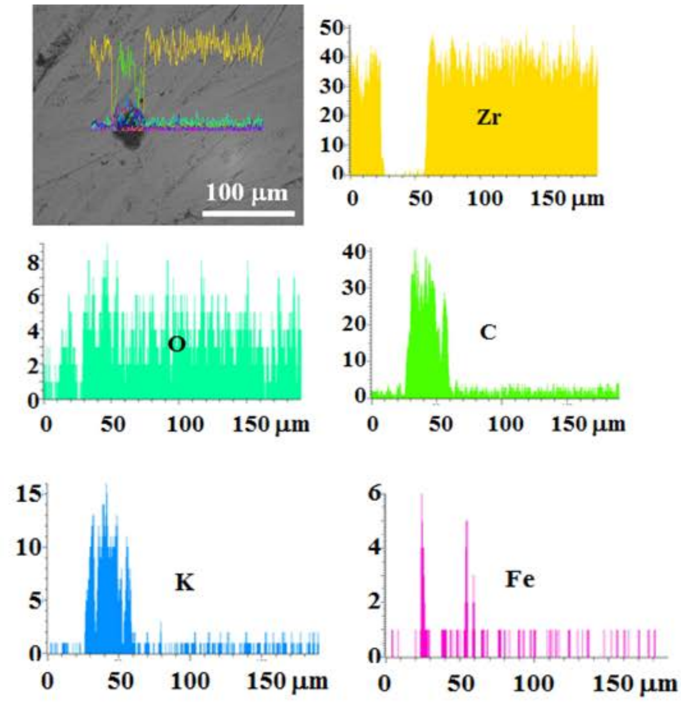

(a)

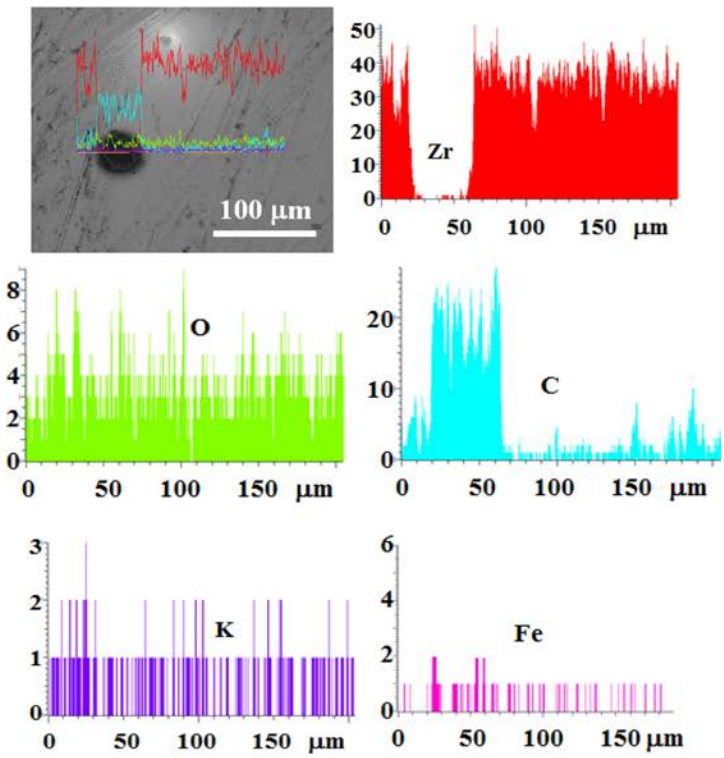

(b)

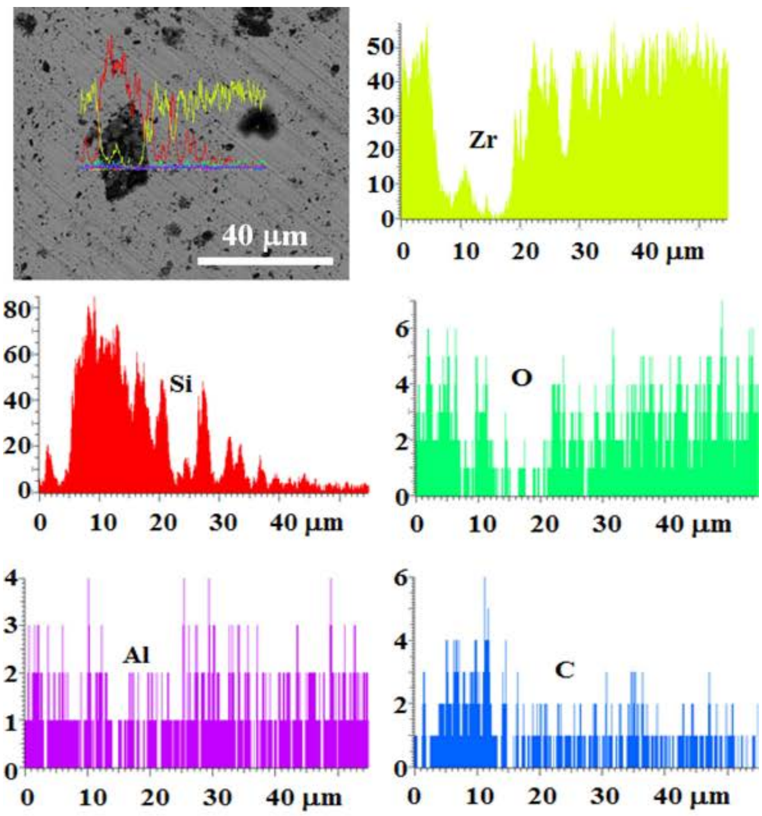

(c)

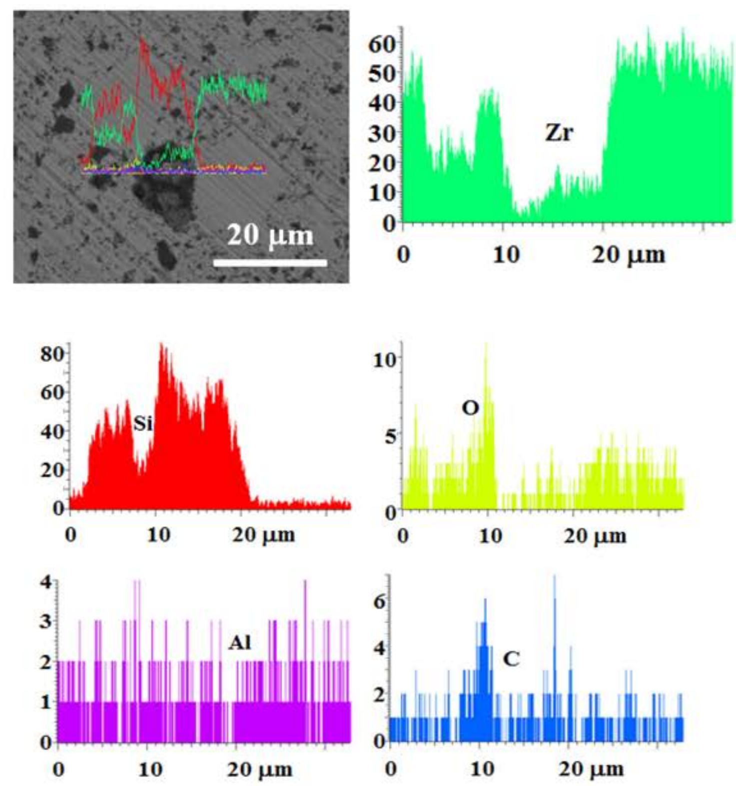

(d)

Fig. 11. Line profiles of the transverse sections of the worn surfaces. (a) As-received Z specimen, (b) 1073K-1h Z specimen, (c) As-received ZS specimen, (d) 1073K-1h ZS specimen.

specimens after wear testing. It was difficult to find worn parts on the counterpart materials. The figure clearly shows the worn parts of the Z and ZS specimens. The worn part reveals the behavior of grinding wear, considering that scratches or stain marks are observed. Grinding wear is a major cause of micro deformation, which accounts for 50% of the causes of wear loss.

After the wear test, further investigation of the worn surface morphologies of the specimens were conducted by SEM. Fig. 9 (a)-(d) show representative as-received Z specimen, 1,073 K-1 h Z specimen, as-received ZS specimen, and 1,073 K-1 h ZS specimen. The as-received Z specimen (a) shows scratches on the surface. The 1,073 K-1 h Z specimen (b) shows scratches on the surface, which are scattered with a large amount of debris combined with indentation defects. This is the result of abrasive adhesion wear. This specimen shows lots of dark regions by heat-treatment. The as-received ZS specimen (c) also displays scratches on the surface. The 1,073 K-1 h ZS specimen (d) also displays scratches on the surface, and shows lots of dark regions by heat-treatment. The ZS specimen does not show debris combined with indentation defects. That is, debris was formed by peeling off the surface layer. The friction coefficient decreased due to the lubricating action of oxide layer, but a severe micro-cutting phenomenon occurred in the contact surface during the dry sliding process. In addition, the light regions (denoted as A) and dark regions (denoted as B) were investigated by EDX.

Fig. 10 shows the result. In the as-received Z specimen (Fig. 10(a)) and the 1,173 K-1 h Z specimen (Fig. 10(b)), the light regions included Zr and O elements, while the dark regions included C, O, Zr, and Fe elements. In the as-received ZS specimen (Fig. 10 (c)) and the 1,173 K-1 h ZS specimen (Fig. 10 (d)), the light regions included Zr and O elements, while the dark regions included C, O, Al, Si, and Fe elements. The dark regions of the heat-treated Z and ZS specimen are the C element, and the debris that is mainly peeled from the counterpart ring; it then underwent a complex formation process of fragmentation, mixing, accumulation, oxidation, compaction, and so forth.

Fig. 11 shows the line profiles of the cross-sections of the as-received Z specimen, the 1,073 K-1 h Z specimen, the as-received ZS specimen and the 1,073 K-1 h ZS specimen. The as-received Z specimen (Fig. 11(a)) displays a bumpy wear surface, wide wear lines, and dark regions. Zr was not detected at all in the dark regions of a measurement distance of (20-60) mm, but was uniformly detected in the light regions. Lots of C and K were detected at (20-60) mm, and O was uniformly present over the entire measurement distance. A small amount of Fe was also detected at a measurement distance of (20 to 60) mm. The 1,073 K-1 h Z specimen (Fig. 11 (b)) was similar to the as-received Z specimen. Zr was not detected at all in a measurement distance of (20-60) mm, and decreased at a measurement distance of (110 and 150) μm. Lots of C was detected at a measurement distance of (20-60) mm, and a small amount was detected at a measurement distance of (110 and 150) mm. Small amounts of K and Fe were also detected. O was uniformly present over the entire measurement distance. The as-received ZS specimen (Fig. 11 (c)) showed narrow wear lines and a large amount of black areas. Zr was hardly detected at the measurement range of (6-18) mm, which is the dark regions, and also decreased at around 28 mm. O showed a tendency similar to Zr. Si and C showed the opposite tendency to Zr. Although Al was small, it was relatively uniformly detected at the entire measurement distance. The 1,073 K-1 h ZS specimen result (Fig. 11 (d)) was similar to the result of the as-received ZS specimen. Ceramic materials are generally subjected not only to brittle fracture under high or impact loads, but also to fatigue cracking induced mainly at grain boundaries by the high surface temperatures and cyclic stresses, generally attained under dry sliding conditions. Under the reciprocating sliding process, the grains beneath the metal mixed particles were fractured, thereby resulting in the formation of micro cracks beneath the metal mixed particles. When the micro cracks propagated, connected, and deflected to the worn surface, the plate-like metal mixed particles were peeled out from the worn surface, and serious wear happened.

Conclusions

In this study, ZrO_2 monolithic ceramics and ZrO_2/SiC composites ceramics were sintered, and heat-treated in air atmosphere of (1,073 and 1,173) K for (1, 5, and 10) h. The as-received specimen and heat-treated specimen were subjected to wear tests. As a result, the following conclusions were obtained.

The mean hardnesses of the as-received Z specimen and as-received ZS specimen were similar. The mean hardness of the heat-treated Z specimen was (2-16) % higher than that of the as-received Z specimen. The mean hardness of the heat-treated ZS specimen was (11-40) % smaller than that of the as-received ZS specimen. This is the effect of glassy SiO_2, which contributes to the crack healing formed on the surface by heat-treatment.

The coefficient of friction of Z and ZS specimens was inversely proportional to the Vickers hardness. The Z specimen was oxidized on the surface by heat-treatment, whereas the ZS specimen formed glass phase SiO_2, which is known as a crack-healing material by the addition of SiC.

The friction coefficient of 9.8 N was greater than that of 24.5 N, despite the lubrication action of surface oxides. However, the friction coefficient of 24.5 N was reduced, because of removing the oxides on the surface, and abrading the surface layer of the ceramic.

The ZS specimen in which the glass phase SiO_2 was forming shows a larger difference in friction coefficient between the two loads.

The wear loss of Z and ZS specimen was not affected by hardness. Wear loss was inversely proportional to hardness. The wear loss and the coefficient of friction of the Z and ZS specimens were proportional. The wear surface showed a scratch or striated pattern, with grinding wear behavior.

References

1. F.F. Lange, J. Amer. ceram. Soc. 53 (1970) 290.
2. A.M. Thompson, H.M. Chan, M.P. Harmer and R.E. Cook, J. Amer. Ceram. Soc. 53 (1995) 567-571.
3. K. Ando, T. Ikeda, S. Sato, F. Yao and Y. Kobayasi, Fatigue & Fracture of Engineering Materials & Structures 21 (1998) 119-122.
4. A.C. Irene, M.C. Helen and P.H. Martin, J. Amer. Ceram. Soc. 81 (1998) 1203-1208.
5. K. Ando, K. Takahashi, S. Nakayama and S. Saito, J. Amer. Ceram. Soc. 85 (2002) 2268-2272.
6. S.K. Lee, W. Ishida, S.Y. Lee, K.W. Nam and K. Ando, J. Euro. Ceram. Soc. 25 (2005) 569-576.
7. C. Zdenek, F. Petr, K. Ando and D. Ivo, J. Euro. Ceram. Soc. 28 (2008) 1073-1077.
8. T. Osada, W. Nakao, K. Takahashi and K. Ando, J. Amer. Ceram. Soc. 92 (2009) 864-869.
9. S.H. Ahn, J.R. Hwang and K.W. Nam, J. Ceram. Process. Res. 15 (2014), 451-456.
10. K. Houjou, K. Ando and K. Takahashi, J. Soc. Mater. Sci. (Jap.) 58 (2009) 510-515.
11. K.W. Nam and J.R. Hwang, J. Mech. Sci. Tech. 26 (2012) 2093-2096.
12. K. Houjou, K. Ando and K. Takahashi, Inter. J. Struct. Integrity. (2010) 73-84.
13. K.W. Nam, Transactions of the KSME(A) 40 (2016) 267-273.
14. A.G. Evans, N. Burlingame, M. Drory and W.M. Kriven, Acta Metallurgica 29 (1981) 447-456.
15. J. Tatami, E. Kodama, H. Watanabe, H. Nakano, T. Wakibara, K. Komeya, T. Meguro and A. Azushima, J. Ceram. Soc. (Jap.) 116 (2008) 749-754.
16. K.W. Nam, Y.K. Chung, S.H. Hwang, J.S. Kim and C.K. Moon, Transactions of the KSME(A) 35 (2011), 267-272.
17. K.W. Nam, J. Ceram. Process. Res.13 (2012), 571-574.
18. S.H. Ahn and K.W. Nam, Transactions of the KSME(A) 38 (2014), 1117-1123.
19. Y. Fu, A.W. Batchelor, H. Xing and Y. Gu, Wear 210 (1997) 157-164.
20. J.H. Ouyang and S. Sasaki, Ceramics International 27 (2001) 251-260.
21. J.F. Li, H. Liao, X.Y. Wang, B. Normand, V. Ji, C.X. Ding and C. Coddet, Tribology International 37 (2004) 77-84.
22. C. Muratore, A.A. Voevodin, J.J. Hu and J.S. Zabinski, Wear 261 (2006) 797-805.
23. J.J. Petrovic, A.K. Bhattacharya, R.E. Honnell, T.E. Mitchell, R.K. Wade and K.J. McClellan, Mater. Sci. Eng. A 155 (1992) 259-266.
24. Y. Zhan and G. Zhang, Tribology Letters 17 (2004) 91-98.
25. M. Nakatani, K. Ando and K. Houjou, J. Euro. Ceram. Soc. 28 (2008) 1251-1257.